

Proton Affinities in Water of Maingroup-Element Hydrides – Effects of Hydration and Methyl Substitution

Marcel Swart,^{[a],†} Ernst Rösler,^[a] and F. Matthias Bickelhaupt^{*[a]}

Keywords: Acidity / Basicity / Density functional calculations / Periodic table / Proton affinities / Thermochemistry / Solvent effects

We have computed the proton affinities in water of archetypal anionic and neutral bases across the periodic table using the generalized gradient approximation (GGA) of density functional theory (DFT) at BP86/QZ4P//BP86/TZ2P. The main purpose of this work is to provide an intrinsically consistent set of values of the 298-K proton affinities in aqueous solution of all anionic (XH_{n-1}^-) and neutral bases (XH_n) constituted by maingroup-element hydrides of groups 14–17 and the noble gases (i.e., group 18) along the periods 1–6. Hy-

dration has little effect on the trends in PA values, especially in the case of the neutral bases. However, in the case of the anionic bases, hydration drastically reduces the magnitude of the PA values. Finally, we have studied how proton affinities in water are affected by methyl substitution at the protophilic center.

(© Wiley-VCH Verlag GmbH & Co. KGaA, 69451 Weinheim, Germany, 2007)

1. Introduction

Designing new (and optimizing existing) approaches and routes in chemical synthesis requires knowledge of the thermochemistry involved in the targeted reactions. In this context, the proton affinity (PA) of a reactant or intermediate species B often plays an important role. This thermochemical quantity is defined as the enthalpy change associated with dissociation of the conjugate acid [Equation (1)].^[1–8]



Overall reaction enthalpies and reaction barriers (and thus reaction rates) are related to the PA, as soon as proton transfer occurs somewhere along the cascade of elementary steps of a reaction mechanism. This is often the case, as proton transfer is ubiquitous in chemical reaction mechanisms, either as simple proton transfer (PT) or as part of a more complex chemical transformation, for example, base-induced elimination reactions that may compete with nucleophilic substitution.^[9–13] And, as chemical reactions are usually carried out in the condensed phase, knowledge of the *condensed-phase* PA values is vital for the understanding and prediction of (competing) reaction mechanisms.

Previously, we have studied the *gas-phase* proton affinities and trends therein of anionic and neutral maingroup-element hydrides and noble gases.^[14,15] Gas-phase proton affinities are obviously directly applicable to gas-phase chemistry^[3–6] but they are also relevant for chemistry occurring in the condensed phase.^[1,16] On one hand, they reveal the intrinsic basicity of the protophilic species involved and, thus, they shed light on how this property is affected by the solvent. On the other hand, they can serve as a universal, solvent-independent framework of reference, from which the actual basicity of a species in solution might be obtained through correcting for the particular solvent under consideration.^[17–19]

Here, we focus on the proton affinities in water and how the presence of the solvent changes the basicity of the protophilic species. The solvent environment may be taken into account using different approximations, e.g., through empirical corrections (Born, Onsager), or by including explicit solvent molecules, or through placing the solute in a dielectric continuum (COSMO^[20,21]). The empirical corrections give only a rough estimate for the solvation process, while the inclusion of explicit solvent molecules necessitates sampling of the solvents' degrees of freedom in molecular simulations^[22,23] (Monte Carlo, molecular dynamics). We choose the dielectric continuum (COSMO^[20,21]) model as a reasonable compromise between accuracy and feasibility.

The present study has three objectives. First, we aim at setting up a complete description at BP86/QZ4P//BP86/TZ2P of the proton affinities ($\text{PA} = \Delta_{\text{acid}} H_{298}$ of reaction 1) in aqueous solution for the anionic ($\text{B} = \text{XH}_{n-1}^-$) and neutral ($\text{B} = \text{XH}_n$) maingroup-element hydrides of groups 14–17 and the noble gases, i.e. group 18, and periods 1–6.

[a] Theoretische Chemie, Scheikundig Laboratorium der Vrije Universiteit, De Boelelaan 1083, 1081 HV Amsterdam, The Netherlands
Fax: +31-20-59-87629
E-mail: fm.bickelhaupt@few.vu.nl

[†] Present address: ICREA (Institut de Recerca i Estudis Avançats) Researcher at Institut de Química Computacional, Universitat de Girona, Campus Montilivi, 17071 Girona, Catalonia, Spain

Supporting information for this article is available on the WWW under <http://www.eurjic.org> or from the author.

In addition to the PA values of all bases ($\Delta_{\text{acid}}H_{298}$), we also report the corresponding 298 K reaction entropies ($\Delta_{\text{acid}}S_{298}$, provided as $-T\Delta_{\text{acid}}S_{298}$ values), and 298 K reaction free energies ($\Delta_{\text{acid}}G_{298}$). We have previously shown that this level of density functional theory (DFT)^[24–32] performs well for computing gas-phase PA values.^[14,15] Second, we wish to evaluate directly the effect of hydration on the PA values by comparing the condensed-phase values to the previously obtained^[14,15] gas-phase values. Third, we examine the influence of stepwise methylation of the protophilic center X in species $\text{Me}_m\text{XH}_{n-m-1}^-$ and $\text{Me}_m\text{XH}_{n-m}$ (for periods 2 and 3), for example, PH_3 , MePH_2 , Me_2PH , Me_3P .

To the best of our knowledge, our series of in total 65 bases has never before been studied consistently with one and the same method over its full range, either experimentally or theoretically. The very consistency in the values of the present study makes our data particularly suitable for inferring accurate *trends* in condensed-phase basicity across the periodic table.

2. Results and Discussion

2.1. Effect of Hydration on Proton Affinities

The computed proton affinities in water (and the corresponding $-T\Delta_{\text{acid}}S_{298}$ and $\Delta_{\text{acid}}G_{298}$ values) of all model

Table 1. Thermodynamic acidity properties (kcal/mol) at $T = 298$ K for anionic bases $\text{Me}_m\text{H}_{n-m}\text{X}^-$ in water.^[a]

Group 14				Group 15				Group 16				Group 17			
Base	ΔH	$-T\Delta S$	ΔG	Base	ΔH	$-T\Delta S$	ΔG	Base	ΔH	$-T\Delta S$	ΔG	Base	ΔH	$-T\Delta S$	ΔG
Period 2															
CH_3^-	220.5	-8.9	211.5	NH_2^-	202.9	-7.5	195.4	OH^-	182.9	-6.6	176.4	F^-	158.1	-5.7	152.4
MeCH_2^-	226.6	-8.9	217.7	MeNH^-	206.6	-7.5	199.1	MeO^-	183.6	-7.1	176.5				
Me_2CH^-	229.7	-8.0	221.7	Me_2N^-	205.1	-7.0	198.1								
Me_3C^-	229.5	-7.2	222.3												
Period 3															
SiH_3^-	193.0	-8.2	184.8	PH_2^-	185.1	-7.5	177.6	SH^-	164.9	-6.4	158.5	Cl^-	143.2	-5.4	137.8
MeSiH_2^-	201.6	-7.6	194.0	MePH^-	192.0	-7.6	184.4	MeS^-	171.2	-6.3	164.8				
Me_2SiH^-	208.3	-7.9	200.4	Me_2P^-	198.2	-7.3	190.9								
Me_3Si^-	213.4	-7.3	206.0												
Period 4															
GeH_3^-	179.4	-8.3	171.2	AsH_2^-	179.8	-7.5	172.3	SeH^-	160.4	-6.3	154.1	Br^-	140.0	-5.2	134.8
Period 5															
SnH_3^-	169.7	-8.1	161.6	SbH_2^-	176.5	-7.5	169.0	TeH^-	158.7	-6.2	152.5	I^-	140.8	-5.1	135.7
Period 6															
PbH_3^-	150.4	-7.0	143.3	BiH_2^-	174.7	-7.4	167.3	PoH^-	157.3	-6.2	151.1	At^-	140.3	-5.0	135.3

[a] Computed at BP86/QZ4P//BP86/TZ2P for the reaction $\text{Me}_m\text{H}_{n-m-1}\text{XH} \rightarrow \text{Me}_m\text{H}_{n-m-1}\text{X}^- + \text{H}^+$ with $n = 3, 2, 1$ and 0 for groups 14, 15, 16 and 17, respectively.

Table 2. Thermodynamic acidity properties (kcal/mol) at $T = 298$ K for neutral bases $\text{Me}_m\text{H}_{n-m}\text{X}$ in water.^[a]

Group 15				Group 16				Group 17				Group 18			
Base	ΔH	$-T\Delta S$	ΔG	Base	ΔH	$-T\Delta S$	ΔG	Base	ΔH	$-T\Delta S$	ΔG	Base	ΔH	$-T\Delta S$	ΔG
Period 1															
												He	35.9	-5.9	30.0
Period 2															
NH_3	160.8	-7.2	153.6	OH_2	127.2	-6.8	120.4	FH	88.7	-6.6	82.1	Ne	39.9	-5.7	34.3
MeNH_2	164.2	-7.6	156.6	MeOH	129.9	-7.5	122.4	MeF	96.5	-6.5	90.0				
Me_2NH	165.2	-7.5	157.6	Me_2O	131.2	-7.1	124.2								
Me_3N	164.7	-7.3	157.5												
Period 3															
PH_3	143.6	-7.2	136.4	SH_2	130.6	-7.5	123.1	ClH	101.5	-6.4	95.1	Ar	68.3	-5.4	62.9
MePH_2	152.7	-7.4	145.4	MeSH	136.9	-7.7	129.2	MeCl	108.3	-6.3	102.0				
Me_2PH	159.3	-7.5	151.8	Me_2S	141.9	-7.8	134.1								
Me_3P	164.2	-7.0	157.2												
Period 4															
AsH_3	131.8	-7.2	124.6	SeH_2	129.6	-7.5	122.1	BrH	103.9	-6.3	97.6	Kr	75.4	-5.3	70.1
Period 5															
SbH_3	127.7	-6.7	121.0	TeH_2	133.6	-6.8	126.7	IH	111.7	-6.2	105.5	Xe	89.3	-5.1	84.2
Period 6															
BiH_3	110.4	-6.6	103.8	PoH_2	133.0	-6.8	126.2	AtH	112.5	-6.2	106.3	Rn	91.8	-5.0	86.7

[a] Computed at BP86/QZ4P//BP86/TZ2P for the reaction $\text{Me}_m\text{H}_{n-m}\text{XH}^+ \rightarrow \text{H}^+ + \text{Me}_m\text{H}_{n-m}\text{X}$ with $n = 3, 2, 1$ and 0 for groups 15, 16, 17 and 18, respectively.

bases are collected in Table 1 and 2 and the trends are visualized in Figure 1. The effect of solvation on the PA values is summarized in Table 3, Table 4 shows the separate contributions from solvation of the base, the proton and the conjugate acid. Before proceeding, we stress that various species for which we compute the proton affinity in water are not stable in water. For example, any anionic base with a

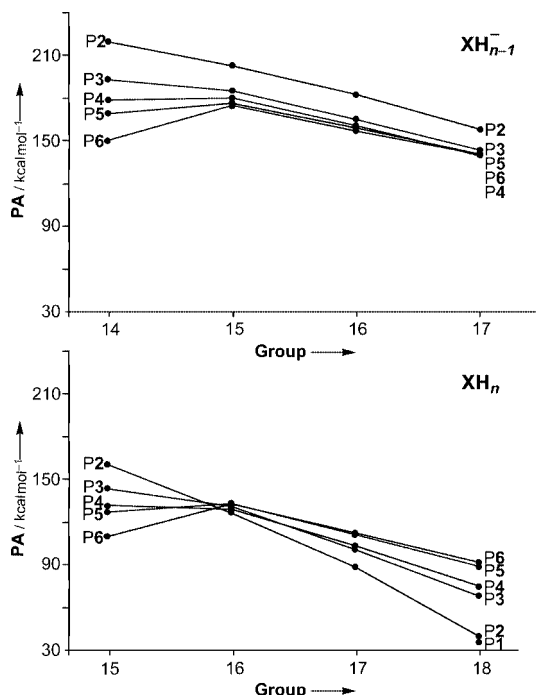


Figure 1. Proton affinities PA in water (at 298 K) of anionic bases XH_{n-1}^- (upper) and neutral bases XH_n (lower) constituted by the element hydrides of groups 14–18 and periods 1–6 (P1–P6), computed at BP86/QZ4P//BP86/TZ2P.

higher PA than that of water (e.g., NH_2^-) will immediately abstract a proton from the latter. Access to the PA value of such in water transient species is interesting both, for the fundamental reason of having a complete trend, but also for the very practical reason to know if such a species remains intact in solution or if it directly abstracts a proton.

Table 4. Enthalpy of hydration (kcal/mol) for bases and their conjugate acids at $T = 298 \text{ K}$.^[a]

Base	$\Delta H_{\text{solv}}(\text{base})$	$\Delta H_{\text{solv}}(\text{conj. acid})$	$\Delta \text{PA}_{\text{solv}}(\text{base})^{[b]}$
CH_3^-	−72.13	1.43	−193.50
NH_2^-	−84.15	−3.39	−200.69
OH^-	−92.22	−4.86	−207.29
F^-	−98.12	−3.51	−214.54
Cl^-	−70.90	−0.50	−190.33
NH_3	−3.39	−80.91	−42.41
OH_2	−4.86	−87.44	−37.35
FH	−3.51	−94.68	−28.76
ClH	−0.50	−85.94	−34.49
Ne	1.45	−105.72	−12.76

[a] Computed at BP86/QZ4P//BP86/TZ2P. [b] See Equation (2). $\Delta H_{\text{solv}}(\text{H}^+) = -119.93 \text{ kcal/mol}$.

Two general observations can be made for the present PA values in aqueous solution by comparison with the corresponding PA values in the gas phase.^[14,15] First, hydration reduces especially the PA values of the anionic bases and somewhat less so the PA values of the neutral bases (see Table 3). Second, the trends in PA values for either the anionic and neutral bases are only little affected by hydration, as follows from comparison of Figure 1 in the present study with that in ref.^[15] (see however also the more detailed discussion in Sections 2.2 and 2.3).

The fact that the neutral bases are much less affected by hydration is easily understood if one considers that the

Table 3. Hydration effects on PA ($\Delta \Delta H$,^[a] kcal/mol) for anionic bases $\text{Me}_m\text{H}_{n-m-1}\text{X}^-$ and neutral bases $\text{Me}_m\text{H}_{n-m}\text{X}$ at $T = 298 \text{ K}$.^[b]

Group 14	Group 15	Group 16	Group 17	Group 15	Group 16	Group 17	Group 18
Base $\Delta \Delta H$	Base $\Delta \Delta H$	Base $\Delta \Delta H$	Base $\Delta \Delta H$	Base $\Delta \Delta H$	Base $\Delta \Delta H$	Base $\Delta \Delta H$	Base $\Delta \Delta H$
Period 1							
Period 2							He −9.3
CH_3^- −193.5	NH_2^- −200.7	OH^- −207.3	F^- −214.6	NH_3 −42.4	OH_2 −37.3	FH −28.7	Ne −12.8
MeCH_2^- −189.0	MeNH^- −191.7	MeO^- −193.0		MeNH_2 −49.8	MeOH −49.3	MeF −46.5	
Me_2CH^- −181.1	Me_2N^- −182.0			Me_2NH −55.3	Me_2O −56.8		
Me_3C^- −174.4				Me_3N −60.3			
Period 3							
SiH_3^- −176.1	PH_2^- −181.1	SH^- −186.5	Cl^- −190.3	PH_3 −41.7	SH_2 −39.6	ClH −34.4	Ar −25.6
MeSiH_2^- −174.6	MePH^- −180.9	MeS^- −186.3		MePH_2 −51.1	MeSH −49.9	MeCl −48.7	
SiH_2^- −172.9	Me_2P^- −179.2			Me_2PH −58.6	Me_2S −58.5		
SiH^- −170.3				Me_3P −64.7			
Period 4							
GeH_3^- −176.5	AsH_2^- −178.3	SeH^- −181.5	Br^- −184.3	AsH_3 −44.8	SeH_2 −42.8	BrH −38.0	Kr −30.7
Period 5							
SnH_3^- −172.3	SbH_2^- −172.0	TeH^- −173.6	I^- −175.1	SbH_3 −47.6	TeH_2 −44.7	IH −40.1	Xe −32.9
Period 6							
PbH_3^- −174.0	BiH_2^- −170.3	PoH^- −171.9	At^- −173.2	BiH_3 −51.0	PoH_2 −47.9	AtH −43.6	Rn −37.4

[a] $\Delta \Delta H$ is the change in PA due to solvation, i.e., $\Delta \text{PA}_{\text{solv}}$, as defined in Equation (2). [b] Computed at BP86/QZ4P//BP86/TZ2P for the reactions $\text{Me}_m\text{H}_{n-m-1}\text{XH} \rightarrow \text{H}^+ + \text{Me}_m\text{H}_{n-m-1}\text{X}^-$ with $n = 3, 2, 1$ and 0 for groups 14, 15, 16 and 17, and $\text{Me}_m\text{H}_{n-m}\text{XH}^+ \rightarrow \text{H}^+ + \text{Me}_m\text{H}_{n-m}\text{X}$ with $n = 3, 2, 1$ and 0 for groups 15, 16, 17 and 18, respectively.

main effect of solvation stems from the ionic species. The change in PA due to solvation, $\Delta\text{PA}_{\text{solv}}$, is given by Equation (2).

$$\Delta\text{PA}_{\text{solv}} = \Delta H_{\text{solv}}(\text{base}) + \Delta H_{\text{solv}}(\text{H}^+) - \Delta H_{\text{solv}}(\text{conj. acid}) \quad (2)$$

The change in enthalpy of solvation of the proton $\Delta H_{\text{solv}}(\text{H}^+)$ is large (-119.93 kcal/mol). For the neutral bases, this term is largely compensated by the strong enthalpy of solvation of their *positively charged conjugate acid*, $\Delta H_{\text{solv}}(\text{conj. acid})$. The latter ranges from -81 to -106 kcal/mol (see Table 4). Consequently, the change in proton affinity due to solvation $\Delta\text{PA}_{\text{solv}}$ is relatively small for neutral bases (see Tables 3 and 4).

The situation is different for the anionic bases. In the gas phase, they have significantly larger PA values than the neutral bases because of the charge separation, and the associated loss in Coulombic attraction, that goes with dissociating the neutral conjugate acid into the negatively charged base and the positively charged proton.^[14,15] On the other hand, in solution, both the base and the proton (but not the conjugate acid) are heavily stabilized as they both carry one elementary charge. Thus, according to Equation (2), there is not a compensation but an amplification of the stabilizing effect of hydration through the terms $\Delta H_{\text{solv}}(\text{base}) + \Delta H_{\text{solv}}(\text{H}^+)$. Consequently, the reduction in proton affinity due to solvation $\Delta\text{PA}_{\text{solv}}$ is large for anionic bases (see Tables 3 and 4).

Eventually, hydration makes the PA values of the anionic bases come closer to those of the neutral bases but they remain somewhat higher than the latter (see Figure 1 and Tables 1 and 2). For instance, the difference in PA between NH_2^- and NH_3 , which is 200 kcal/mol in the gas phase, is reduced to 42 kcal/mol in water (see Tables 1 and 2). This is mainly due to the PA of the *anionic* base (NH_2^-) that decreases by 201 kcal/mol, while that of the *neutral* base (NH_3) decreases by only 42 kcal/mol (see Table 3).

2.2. Trends in Proton Affinities in Water

The *trends* in PA values for either the anionic and neutral bases are, as pointed out above, much less affected by hydration than the absolute values. Yet there are small but not negligible effects which are discussed in the present section. Furthermore, we note that hydration effects on trends in PA values are only small in the case of the simple element hydrides. Later on, in Section 2.3, we will see that trends can in fact be qualitatively changed by hydration in the case of the methyl-substituted bases.

First, we examine the trends in PA values in water as such before we consider the changes relative to the gas phase. For the anionic bases, we obtain the well-known trend of a decreasing basicity along the second period as the PA falls from 221 to 203 to 183 to 158 kcal/mol along CH_3^- , NH_2^- , OH^- and F^- (see Table 1 and Figure 1). The PA values also decrease down each group: for instance, for group 15, the PA decreases from 203 to 185 to 180 to 177 to 175 kcal/mol along NH_2^- , PH_2^- , AsH_2^- , SbH_2^- and BiH_2^- .

However, the changes in descending group 14 are significantly larger than those in groups 15–17. Thus, as can be seen in Figure 1, upper, the trend for monotonic decrease in PA along the second (P2) and third (P3) periods changes into a trend where the PA first increases from group 14 to group 15 and then decreases again along groups 15, 16 and 17. The corresponding reaction entropies yield a relatively small (but not entirely constant) contribution $-T \Delta_{\text{acid}} S_{298}$ of -5 to -9 kcal/mol for 298 K. As a consequence, the Gibbs free energies $\Delta_{\text{acid}} G_{298}$ show the same trends as the corresponding PA values (see Table 1).

For the neutral bases, we also obtain the well-known trend of decreasing basicity along the second period, just as for the anionic bases. Thus, the PA falls from 161 to 127 to 89 to 40 for NH_3 , OH_2 , FH , Ne . A striking change occurs from group 15 to groups 17 and 18. Descending group 15, the PA *decreases* but descending groups 17 and 18, the PA *increases* (see Table 2). Group 16 is an intermediate case with relatively constant PA values that do not show a pronounced trend. Thus, the trend of monotonic decrease of PA along the second (P2), third (P3), and fourth (P4) period changes into a trend, along the fifth (P5) and sixth (P6) period, of an initial increase of the PA from group 15 to group 16 followed by a decrease along groups 16–18 (see Figure 1, lower).

There is an interesting common feature in the trends of both anionic and neutral bases. This feature is the kink in the PA trend along a period that always occurs after the step from the tricoordinate to the dicoordinate base, that is, at group 15 for the anionic XH_{n-1}^- and at group 16 for the neutral XH_n (see Figure 1). The effect is most pronounced for bases with a more heavy protophilic center in which the valence *ns* AO is inactive. This suggests that the effect, that is, the sudden increase in PA from a tricoordinate to a dicoordinate base is associated with an active *np*-type lone pair which becomes available in the latter.

The above trends of PA values in water are very similar to those in the gas phase. But, as announced above, there are differences which manifest themselves in particular in the case of the anionic bases. In the first place, the *magnitude of the hydration effect* (ΔPA) on the PA values of the anionic bases XH_{n-1}^- strongly *decreases down each group* (see Table 3). The largest change occurs from period 2 to period 3. This causes the PA values of XH_{n-1}^- from different periods to shift closer together. The decrease in the hydration effect ΔPA on the proton affinities if one descends the periodic Table can be easily understood with the classical electrostatic Born model of a spherical ion in a dielectric continuum [Equation (3), in a.u.].^[17,33]

$$\Delta E_{\text{solv}} = -\frac{q^2}{2a} \left(1 - \frac{1}{\epsilon_r} \right) \quad (3)$$

In this equation, ϵ_r is the relative dielectric constant of the solvent (i.e. 78.4 for water). The charge q is -1 for the XH_{n-1}^- ion. The appearance of the effective radius a of the

ion in the denominator leads to smaller solvation energies for larger ions. Thus, as the atomic radius of the protophilic center X (and therefore of the base XH_{n-1}^-) increases down a group, the stabilization due to solvation of the anionic base $\Delta\Delta H_{\text{solv}}(\text{base})$ diminishes and so does, according to Equation (2), the hydration effect ΔPA on the proton affinity.

The same simple model (i.e. Equations 2 and 3) predicts that, in the case of the neutral bases, the hydration effect increases down the periodic Table. This is indeed what happens although the effect is somewhat less pronounced than that for the anionic bases (see Table 3). Similar size effects can also be observed along a period. For example, the hydration-induced reduction of the proton affinity, ΔPA , increases from -194 to -201 to -207 to -215 kcal/mol along CH_3^- , NH_2^- , OH^- and F^- (see Table 3). In fact, the value of -214.6 kcal/mol for F^- is the largest hydration effect on a PA value in this study. The trend in ΔPA along the second period anionic bases can again be understood in terms of the solvation stabilization becoming more effective as the anionic protophilic center becomes smaller (see equations 2 and 3).

2.3. Methyl Substituent Effects

Finally, we have studied the effect on the PA in water of stepwise replacing all hydrogen atoms in second- and third-period anionic bases XH_{n-1}^- and neutral bases XH_n by methyl substituents, for which the results are collected in Tables 1, 2 and 5 and visualized in Figures 2 and 3. Methyl substitution increases the basicity in aqueous solution as reflected by the PA in all cases, that is, for both second- and

third-period anionic and neutral bases. For example, along OH_2 , MeOH and Me_2O , the PA increases from 127 to 130 to 131 kcal/mol, and along SH_2 , MeSH and Me_2S , the PA increases from 131 to 137 to 142 kcal/mol (see Table 2). In three cases the trend comes practically to a hold along the step in which the last possible methyl group is introduced, namely, from Me_2CH^- to Me_3C^- , from MeNH^- to Me_2N^- and from Me_2NH to Me_3N (see Tables 1 and 2).

This similarity in PA trends between second- and third-period bases in water contrasts with the situation for the anionic bases in the gas phase.^[14,15] In the case of the latter, methyl substitution also increases the PA of third-period bases XH_{n-1}^- but it *decreases* the PA of the second-period bases XH_{n-1}^- . It was shown that the reduction in basicity of the second-period anionic bases is *not* the result of a stabilization of the protophilic center by methyl groups.^[14] In fact, the introduction methyl groups *destabilizes in all cases* both the base and the conjugate acid. The opposite trends in the effect of methyl substitution on the gas-phase PA of second- and third-period anionic bases XH_{n-1}^- originate from the fact that a *second-period base is destabilized less by introducing a methyl group* than its corresponding conjugate acid whereas a *third-period base is destabilized more* than its conjugate acid.

This difference between methyl-substituent effects on the PA of second- and third-period anionic bases obviously disappears in aqueous solution. Our analyses show that this is associated with the loss in solute–solvent interaction that goes with methyl substitution. The anionic second-period bases are particularly strongly solvated [due to the small size of their charged protophilic center, see Equation (3)], significantly more so than their neutral conjugate acid.

Table 5. Analysis of the methyl-substituent effect on PA energies $\Delta_{\text{acid}}E$ in water in terms of the partial reaction schemes in Figure 2 and Figure 3.^[a]

Base	$\Delta E_{\text{N/C}}$	$\Delta E_{\text{A/N'}}$	$\Delta_{\text{acid}}E$	Base	ΔE_{C}	$\Delta E_{\text{N'}}$	$\Delta_{\text{acid}}E$
C^{3-}			158.02	Si^{3-}			147.17
CH_3^-	-360.50	-289.77	228.75	SiH_3^-	-293.12	-241.87	198.42
MeCH_2^-	-341.36	-264.66	234.72	MeSiH_2^-	-285.72	-226.07	206.82
Me_2CH^-	-323.61	-243.73	237.90	Me_2SiH^-	-277.99	-211.76	213.40
Me_3C^-	-306.55	-226.48	238.09	Me_3Si^-	-270.18	-198.98	218.37
N^{3-}			201.26	P^{3-}			191.23
NH_2^-	-222.46	-213.11	210.61	PH_2^-	-172.78	-173.91	190.10
MeNH^-	-194.99	-181.56	214.69	MePH^-	-158.51	-152.70	197.04
Me_2N^-	-170.46	-157.70	214.02	Me_2P^-	-145.63	-133.69	203.17
O^{2-}			180.63	S^{2-}			168.19
OH^-	-129.99	-121.34	189.28	SH^-	-97.85	-96.90	169.14
MeO^-	-98.75	-88.39	190.99	MeS^-	-78.50	-71.02	175.67
N^{3-}			61.29	P^{3-}			84.56
NH_3	-425.33	-317.38	169.24	PH_3	-317.23	-252.25	149.54
MeNH_2	-401.11	-289.91	172.49	MePH_2	-311.45	-237.98	158.03
Me_2NH	-377.62	-265.38	173.53	Me_2PH	-305.21	-225.10	164.67
Me_3N	-354.46	-242.56	173.19	Me_3P	-298.41	-213.46	169.51
O^{2-}			100.48	S^{2-}			131.37
OH_2	-280.48	-246.69	134.27	SH_2	-194.39	-189.73	136.03
MeOH	-252.05	-215.45	137.08	MeSH	-181.40	-170.38	142.39
Me_2O	-225.94	-187.76	138.66	Me_2S	-169.05	-153.01	147.41
F^-			69.33	Cl^-			100.12
FH	-174.48	-149.90	93.91	ClH	-116.06	-110.52	105.66
MeF	-152.63	-119.88	102.08	MeCl	-101.25	-88.53	112.84

[a] Computed at BP86/QZ4P//BP86/TZ2P.

Therefore, these bases also suffer most from the shielding of the charged protophilic center from the solvent by the methyl substituents. Consequently, in water, methyl-substitution destabilizes the base more than it destabilizes the conjugate acid also in the case of the anionic second-period bases.

This leads to the well-known reversal, from gas phase to condensed phase, of the trend in basicity along a series of increasingly methyl-substituted second-period bases. For example, in the gas phase, the basicity decreases along $\text{OH}^- > \text{MeO}^-$ and along $\text{NH}_2^- > \text{MeNH}^- > \text{Me}_2\text{N}^-$. But in water, the basicity decreases in the opposite order, namely, along $\text{MeO}^- > \text{OH}^-$ and along $\text{Me}_2\text{N}^- > \text{MeNH}^- > \text{NH}_2^-$ (see Table 1 and ref.^[14]).

Our analyses that lead to the above conclusion consist of a decomposition of the proton-affinity energies $\Delta_{\text{acid}}E$ [i.e., only the electronic-energy part, ΔE , of the proton affinity, see Equation (6) in methodological section], associated with acid dissociation of the conjugate acids, into three partial reactions, as shown in the thermochemical cycles in the top panels of Figures 2 and 3. This decomposition is now ex-

plained for the anionic bases [see Equation (4)] but the situation is of course completely equivalent for the neutral bases [see Equation (5)]. The first step, which is associated with an energy change $-\Delta E_{\text{N}}(m)$, is dissociation of all substituents (but not the acidic proton) of the conjugate acid $\text{Me}_m\text{H}_{n-m-1}\text{XH}$ to form the radical $\text{XH}^{(n-1)\cdot}$ (see Figure 2). The energy $\Delta E_{\text{N}}(m)$ is the stabilization of the protophilic center X in the neutral conjugate acid $\text{Me}_m\text{H}_{n-m-1}\text{XH}$ by all substituents, i.e., the interaction with m methyl groups (Me) and $n-m-1$ hydrogen atoms (H). Next, the unsubstituted acid $\text{XH}^{(n-1)\cdot}$ is dissociated into $\text{X}^{-(n-1)\cdot} + \text{H}^+$ (see Figure 2). The corresponding reaction energy is the proton-affinity energy $\Delta_{\text{acid}}E$ of the anionic base $\text{X}^{-(n-1)\cdot}$. The third and last step, which is associated with an energy change $\Delta E_{\text{A}}(m)$, is addition of all substituents to the protophilic center $\text{X}^{-(n-1)\cdot}$ to form the base $\text{Me}_m\text{H}_{n-m-1}\text{X}^-$ (see Figure 2; m = number of methyl substituents). The energy $\Delta E_{\text{A}}(m)$ is the stabilization of the protophilic center X in the anionic base $\text{Me}_m\text{H}_{n-m-1}\text{X}^-$ by all substituents, i.e., the interaction with m methyl groups (Me) and $n-m-1$ hydrogen atoms (H). The computed proton-affinity energies $\Delta_{\text{acid}}E$, ΔE_{N} and

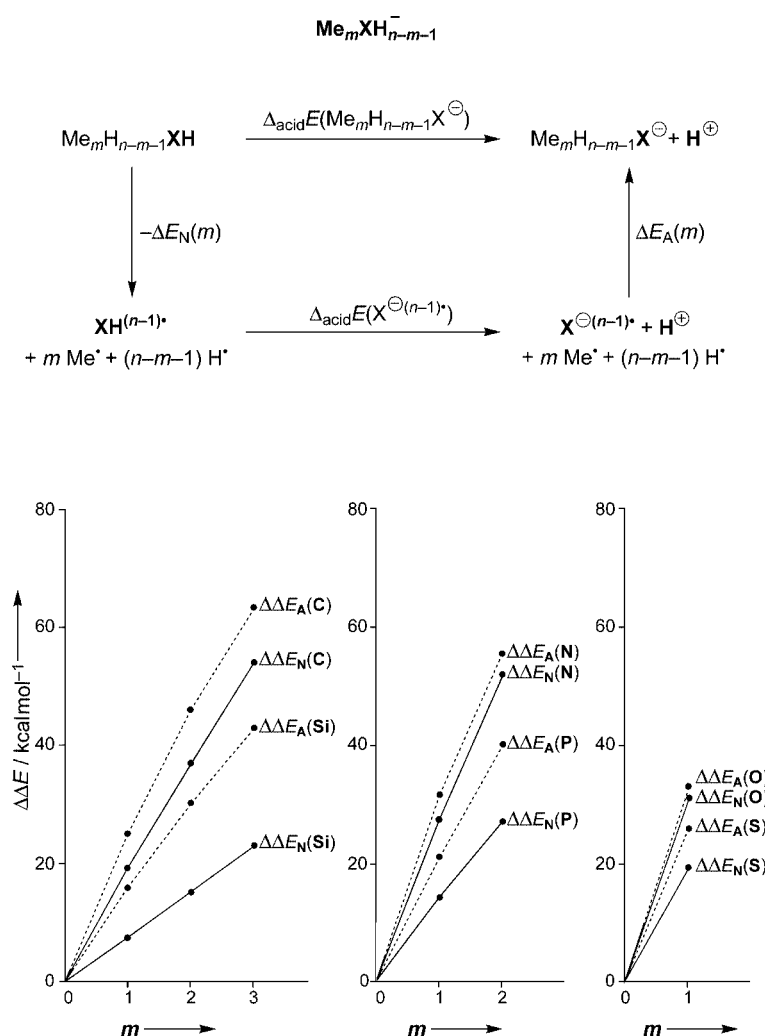


Figure 2. Effect of methyl substitution on the energies $\Delta E_{\text{N}}(\text{X})$ and $\Delta E_{\text{A}}(\text{X})$ of the anionic XH_{n-1}^- and corresponding neutral conjugate acids XH_n in water, computed at BP86/QZ4P/BP86/TZ2P [see Equation (4) and Table 5].

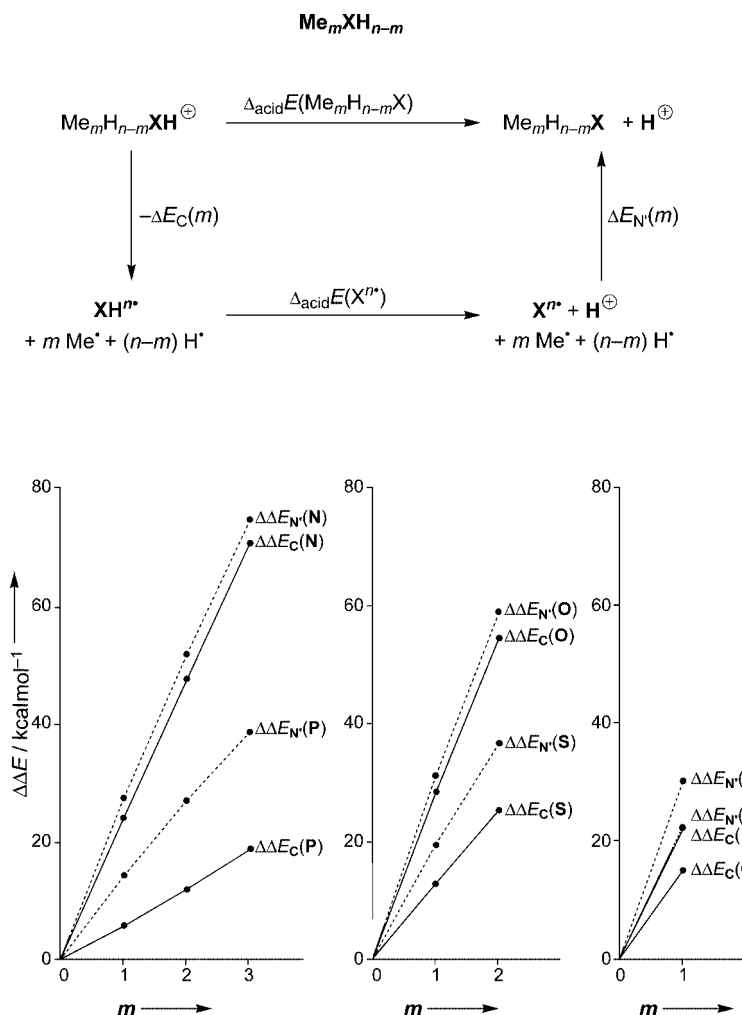


Figure 3. Effect of methyl substitution on the energies $\Delta E_{\text{C}}(\text{X})$ and $\Delta E_{\text{N}'}(\text{X})$ of the neutral XH_n and corresponding cationic conjugate acids XH_{n+1}^+ in water, computed at BP86/QZ4P//BP86/TZ2P [see Equation (5) and Table 5].

ΔE_{A} of the *anionic* bases are collected in Table 5, together with corresponding energy terms $\Delta_{\text{acid}}E$, ΔE_{C} and $\Delta E_{\text{N}'}$ for the *neutral* bases.

The relationship between the proton-affinity energy $\Delta_{\text{acid}}E$ and the other energy terms of the thermochemical cycles shown in Figures 2 and 3 is summarized in Equations (4) and (5) (m = number of methyl substituents) for the anionic ($\text{Me}_m\text{H}_{n-m-1}\text{X}^-$) and the neutral bases ($\text{Me}_m\text{H}_{n-m}\text{X}$).

$$\Delta_{\text{acid}}E(\text{Me}_m\text{H}_{n-m-1}\text{X}^-) = \Delta_{\text{acid}}E(\text{X}^{-(n-1)*}) + \Delta E_{\text{A}}(m) - \Delta E_{\text{N}}(m) \quad (4)$$

$$\Delta_{\text{acid}}E(\text{Me}_m\text{H}_{n-m}\text{X}) = \Delta_{\text{acid}}E(\text{X}^{n*}) + \Delta E_{\text{N}'}(m) - \Delta E_{\text{C}}(m) \quad (5)$$

Thus, according to Equation (4), the proton-affinity energy $\Delta_{\text{acid}}E(\text{Me}_m\text{H}_{n-m-1}\text{X}^-)$ of the base $\text{Me}_m\text{H}_{n-m-1}\text{X}^-$ is determined by the proton-affinity energy $\Delta_{\text{acid}}E(\text{X}^{-(n-1)*})$ of the unsubstituted and deprotonated protophilic center $\text{X}^{-(n-1)*}$ plus the *difference* in stabilization $\Delta E_{\text{A}}(m)$ of $\text{X}^{-(n-1)*}$ in the base $\text{Me}_m\text{H}_{n-m-1}\text{X}^-$ and the stabilization

$\Delta E_{\text{N}}(m)$ of $\text{XH}^{(n-1)*}$ in $\text{Me}_m\text{H}_{n-m-1}\text{XH}$ by m methyl (Me) and $n-m-1$ hydrogen substituents. The methyl-substituent effect on the proton-affinity energy, i.e., the change $\Delta\Delta_{\text{acid}}E(m)$ in this value if one goes from 0 to m methyl substituents, therefore depends not only on the change $\Delta E_{\text{A}}(m) - \Delta E_{\text{A}}(0)$ in stabilization of the anionic base *but also on the change* $\Delta E_{\text{N}}(m) - \Delta E_{\text{N}}(0)$ in stabilization of the *neutral conjugate acid*. And, the same holds, *mutatis mutandis*, for the neutral bases, see Equation (5).

In Figure 2, lower panel, we have plotted the changes in stabilization by the substituents $\Delta\Delta E_{\text{A}} = \Delta E_{\text{A}}(m) - \Delta E_{\text{A}}(0)$ and $\Delta\Delta E_{\text{N}} = E_{\text{N}}(m) - \Delta E_{\text{N}}(0)$ for the anionic second- and third-period bases $\text{Me}_m\text{H}_{n-m-1}\text{X}^-$ and their conjugate acids $\text{Me}_m\text{H}_{n-m-1}\text{XH}$. In the lower panel of Figure 3, the corresponding plots for the neutral bases are depicted. Now it is clear that introducing a methyl substituent, i.e., replacing a hydrogen by the sterically more demanding and solvent-shielding methyl group, leads consistently in all cases to a destabilization of the system. And, contrasting the situation for the anionic bases in the gas-phase,^[14] a methyl group

destabilizes the anionic base more than its corresponding neutral conjugate acid also for the second period and not only the third period.

3. Conclusions

The proton affinities (PA) in water of simple anionic bases XH_{n-1}^- and neutral bases XH_n (derived from or constituted by main-group-element hydrides XH_n) show qualitatively similar trends along a period or down a group in the periodic table as the corresponding PA values in the gas phase, namely: a monotonic decrease along the second and third period which starting at the fourth (for XH_{n-1}^-) or fifth period (for XH_n) turns into a peak-shaped trend with an initial increase from the tri- to the dicoordinate base (e.g. from GeH_3^- to AsH_2^-) followed again by a monotonic decrease along the rest of the period.

In the gas phase, the anionic bases XH_{n-1}^- have a significantly higher PA than the neutral bases XH_n . Hydration however drastically reduces the PA of the anionic bases, i.e., much more so than that of the neutral bases. This causes the PA values of anionic and neutral bases to differ much less in aqueous solution than in the gas phase.

In water, methyl substitution increases practically always the PA of both the anionic bases $\text{Me}_m\text{XH}_{n-m-1}^-$ and the neutral bases $\text{Me}_m\text{XH}_{n-m}$. In the gas phase, methyl substitution has the same effect with one important exception: in the case of the anionic second-period bases $\text{Me}_m\text{XH}_{n-m-1}^-$, the gas-phase PA decreases if methyl groups are introduced. Thus, for example, OH^- is more basic than MeO^- in the gas phase but, in water, MeO^- is more basic than OH^- . We have analyzed in detail why this is so.

4. Methods

4.1. Basis Sets

All calculations were performed with the Amsterdam Density Functional (ADF) program.^[34,35] Molecular orbitals (MOs) were expanded using two different large, uncontracted sets of Slater-type orbitals: TZ2P and QZ4P.^[36] The TZ2P basis is of triple- ζ quality, augmented by two sets of polarization functions (2*p* and 3*d* on H; *d* and *f* on heavy atoms). The QZ4P basis, which contains additional diffuse functions, is of quadruple- ζ quality, augmented by four sets of polarization functions (two 2*p* and two 3*d* sets on H; two *d* and two *f* sets on heavy atoms). Core electrons (e.g. 1*s* for 2nd period, 1*s*2*s*2*p* for 3rd period, 1*s*2*s*2*p*3*s*3*p* for 4th period, 1*s*2*s*2*p*3*s*3*p*3*d*4*s*4*p* for 5th period, 1*s*2*s*2*p*3*s*3*p*3*d*4*s*4*p*4*d* for 6th period) were treated by the frozen core (FC) approximation.^[35] An auxiliary set of *s*, *p*, *d*, *f*, and *g* STOs was used to fit the molecular density and to represent the Coulomb and exchange potentials accurately in each SCF cycle. Scalar relativistic corrections were included self-consistently using the Zeroth Order Regular Approximation (ZORA).^[37]

4.2. Density Functional

Energies and gradients were calculated using the local density approximation (LDA; Slater exchange and VWN^[38] correlation) with gradient corrections^[31,32] due to Becke (exchange) and Perdew (correlation) added self-consistently. This is the BP86 density func-

tional, which is one of the three best DFT functionals for the accuracy of geometries,^[39] with an estimated unsigned error of 0.009 Å in combination with the TZ2P basis set. In a previous study^[14] on the proton affinity of anionic species, we compared the energies of a range of other DFT functionals, to estimate the influence of the choice of DFT functional. These functionals included the Local Density Approximation (LDA), Generalized Gradient Approximations (GGAs), *meta*-GGA and hybrid functionals. The BP86 functional emerged as one of the best functionals. The restricted and unrestricted formalisms were used for closed-shell and open-shell species, respectively. In the present study, all geometry optimizations and vibrational analyses have been done at BP86/TZ2P. Energies have been computed in a single-point fashion, on top of the BP86/TZ2P geometries, using the BP86/QZ4P level of theory. Overall, this leads to a BP86/QZ4P//BP86/TZ2P approach.

4.3. Solvent Effects and Thermochemistry

Solvent effects were taken into account in all calculations using the COSMO model,^[20,21] used explicitly both within the solving of the SCF equations and the optimization of the geometry. The solvent radius (R_s) for water was taken from experimental data for the macroscopic density (ρ) and molecular mass (M_m) with the formula $R_s^3 = 2.6752 \cdot M_m / \rho$,^[40] leading to a R_s value of 1.9 Å for water; a value of 78.4 was used for the dielectric constant of water. Atomic radii values were taken from the MM3 van der Waals radii,^[41] which are available for almost the whole periodic system, and scaled by 0.8333 (the MM3 radii are 20% larger than the normal van der Waals radii due to the specific form for the van der Waals energy within the MM3 force field). The surface charges at the GEPOL93 solvent-excluding surface^[42–44] were corrected for outlying charges. This setup provides a “non-empirical” approach to including solvent effects with a dielectric continuum, and works well for solvation processes.^[1] The file needed for including this setup in a COSMO computation with the ADF program (including all values of the above-mentioned atomic radii) is provided as Table S1 in the electronic supporting information.

Geometries were optimized using analytical gradient techniques until the maximum gradient component was less than 1.0×10^{-4} atomic units (see Table S2 in the electronic supporting information). Vibrational frequencies were obtained through numerical differentiation of the analytical gradients,^[35] where for most of the systems the GEPOL93 surface was recreated at each displaced geometry.

For three systems (i.e., Me_3N , Me_3NH^+ and Me_3PH^+), these standard settings resulted in one large imaginary frequency (in the range from -2300 to -24000 cm^{-1}) which, however, proved to have a positive value (of around 1200 and 2000 cm^{-1}) in the more accurate (automatic) PES scan afterwards. This imaginary frequency is related to the numerical differentiation in combination with the GEPOL93 surface. Thus, by creating the GEPOL93 surface in the case of the three problematic systems *only* for the initial geometry and keeping this surface (geometrically) fixed for all displaced geometries, the large imaginary frequencies do not occur. Moreover, for well-behaved systems, keeping the GEPOL93 surface fixed or recreating them at every displaced geometry has a negligible effect on the enthalpy ($<0.1 \text{ kcal/mol}$). Thus, for the problematic cases of Me_3N , Me_3NH^+ and Me_3PH^+ , we used the thermodynamic data from the calculations where the GEPOL93 surface was fixed.

Reaction enthalpies at 298.15 K and 1 atm (ΔH_{298}) were calculated from the corresponding changes in electronic energy (ΔE) according to Equation (6), assuming an ideal gas.^[33]

$$\Delta H_{298} = \Delta E + \Delta E_{\text{trans},298} + \Delta E_{\text{rot},298} + \Delta E_{\text{vib},0} + \Delta(\Delta E_{\text{vib}})_{298} + \Delta(pV) \quad (6)$$

Here, $\Delta E_{\text{trans},298}$, $\Delta E_{\text{rot},298}$ and $\Delta E_{\text{vib},0}$ are the differences between products and reactants in translational, rotational and zero point vibrational energy, respectively; $\Delta(\Delta E_{\text{vib}})_{298}$ is the change in the vibrational energy difference as one goes from 0 to 298.15 K. The vibrational energy corrections are based on our frequency calculations. The molar work term for the gas-phase process, $\Delta(pV)$, is taken to be $(\Delta n)RT$; $\Delta n = +1$ for one reactant BH^+ dissociating into two products $\text{B} + \text{H}^+$. Thermal corrections for the electronic energy are neglected.

Supporting Information (see also the footnote on the first page of this article): Figures S1–S3 in color, input file (including atomic radii) for “non-empirical” COSMO solvation computations with ADF, and Cartesian coordinates of all species occurring in this study.

Acknowledgments

We thank the Netherlands organization for Scientific Research (NWO-CW) for financial support.

- [1] R. S. Bon, B. van Vliet, N. E. Sprenkels, R. F. Schmitz, F. J. J. de Kanter, C. V. Stevens, M. Swart, F. M. Bickelhaupt, M. B. Groen, R. V. A. Orru, *J. Org. Chem.* **2005**, *70*, 3542–3553.
- [2] J.-F. Gal, P.-C. Maria, E. D. Raczynska, *J. Mass Spectrom.* **2001**, *36*, 699–716.
- [3] E. P. L. Hunter, S. G. Lias, *J. Phys. Chem. Ref. Data* **1998**, *27*, 413–656.
- [4] S. G. Lias, J. E. Bartmess, J. F. Liebman, J. L. Holmes, R. D. Levin, W. G. Mallard, *J. Phys. Chem. Ref. Data* **1988**, *17*, Suppl. No. 1.
- [5] J. E. Szulejko, T. B. McMahon, *J. Am. Chem. Soc.* **1993**, *115*, 7839–7848.
- [6] B. J. Smith, L. Radom, *J. Am. Chem. Soc.* **1993**, *115*, 4885–4888.
- [7] K. E. Bartmess, J. A. Scott, R. T. McIver Jr, *J. Am. Chem. Soc.* **1979**, *101*, 6046–6056.
- [8] S. T. Graul, R. R. Squires, *J. Am. Chem. Soc.* **1990**, *112*, 2517–2529.
- [9] F. M. Bickelhaupt, *Mass Spectrom. Rev.* **2001**, *20*, 347–361.
- [10] F. M. Bickelhaupt, E. J. Baerends, N. M. M. Nibbering, T. Ziegler, *J. Am. Chem. Soc.* **1993**, *115*, 9160–9173.
- [11] F. M. Bickelhaupt, G. J. H. Buisman, L. J. de Koning, N. M. M. Nibbering, E. J. Baerends, *J. Am. Chem. Soc.* **1995**, *117*, 9889–9899.
- [12] F. M. Bickelhaupt, G. J. H. Buisman, L. J. de Koning, N. M. M. Nibbering, E. J. Baerends, *J. Am. Chem. Soc.* **1996**, *118*, 1579–1579.
- [13] F. M. Bickelhaupt, L. J. de Koning, N. M. M. Nibbering, *J. Org. Chem.* **1993**, *58*, 2436–2441.
- [14] M. Swart, F. M. Bickelhaupt, *J. Chem. Theory Comput.* **2006**, *2*, 281–287.
- [15] M. Swart, E. Rösler, F. M. Bickelhaupt, *J. Comput. Chem.* **2006**, *27*, 1486–1493.
- [16] F. M. Bickelhaupt, E. J. Baerends, N. M. M. Nibbering, *Chem. Eur. J.* **1996**, *2*, 196–207.
- [17] M. Born, *Z. Phys.* **1920**, *1*, 45–48.
- [18] L. Onsager, *J. Am. Chem. Soc.* **1936**, *58*, 1486–1493.
- [19] M. W. Wong, M. J. Frisch, K. B. Wiberg, *J. Am. Chem. Soc.* **1991**, *113*, 4776–4782.
- [20] A. Klamt, G. Schüürmann, *J. Chem. Soc. Perkin Trans. 2* **1993**, 799–805.
- [21] C. C. Pye, T. Ziegler, *Theor. Chem. Acc.* **1999**, *101*, 396–408.
- [22] M. P. Allen and D. J. Tildesley, *Computer Simulation of Liquids*, Clarendon Press, Oxford, **1987**.
- [23] D. Frenkel, B. Smit, *Understanding molecular simulation: from algorithms to applications*, Academic Press, **1996**.
- [24] R. Dreizler, E. Gross, *Density Functional Theory*, Plenum Press, New York, **1995**.
- [25] W. Koch, M. C. Holthausen, *A Chemist's Guide to Density Functional Theory*, Wiley-VCH, Weinheim, **2000**.
- [26] R. G. Parr, W. Yang, *Density functional theory of atoms and molecules*, Oxford University Press, New York, **1989**.
- [27] M. Ernzerhof, J. P. Perdew, K. Burke in *Density functionals: Where do they come from, why do they work?*, vol. 180 (Ed.: R. F. Nalejowski), Springer, Berlin, **1996**, pp. 1–30.
- [28] S. Kurth, J. P. Perdew, P. Blaha, *Int. J. Quantum Chem.* **1999**, *75*, 889–909.
- [29] J. P. Perdew, A. Ruzsinszky, J. M. Tao, V. N. Staroverov, G. E. Scuseria, G. I. Csonka, *J. Chem. Phys.* **2005**, *123*, 062201.
- [30] J. P. Perdew, J. M. Tao, V. N. Staroverov, G. E. Scuseria, *J. Chem. Phys.* **2004**, *120*, 6898–6911.
- [31] J. P. Perdew, *Phys. Rev. B* **1986**, *33*, 8822–8824. Erratum: *Phys. Rev. B* **1986**, *33*, 8834, 7406.
- [32] A. D. Becke, *Phys. Rev. A* **1988**, *38*, 3098.
- [33] P. W. Atkins, *Physical Chemistry*, Oxford University Press, Oxford, **1994**, p.
- [34] E. J. Baerends, J. Autschbach, A. Bérces, C. Bo, P. L. de Boeij, P. M. Boerrigter, L. Cavallo, D. P. Chong, L. Deng, R. M. Dickson, D. E. Ellis, L. Fan, T. H. Fischer, C. Fonseca Guerra, S. J. A. van Gisbergen, J. A. Groeneveld, O. V. Gritsenko, M. Grüning, F. E. Harris, P. van den Hoek, H. Jacobsen, G. van Kessel, F. Kootstra, E. van Lenthe, D. A. McCormack, A. Michalak, V. P. Osinga, S. Patchkovskii, P. H. T. Philipsen, D. Post, C. C. Pye, W. Ravenek, P. Ros, P. R. T. Schipper, G. Schreckenbach, J. G. Snijders, M. Solà, M. Swart, D. Swerhonne, G. te Velde, P. Vernooijs, L. Versluis, O. Visser, F. Wang, E. van Wezenbeek, G. Wiesenekker, S. K. Wolff, T. K. Woo, A. L. Yakovlev, T. Ziegler, *ADF 2005.01*, SCM, Amsterdam, **2005**.
- [35] G. te Velde, F. M. Bickelhaupt, E. J. Baerends, C. Fonseca Guerra, S. J. A. van Gisbergen, J. G. Snijders, T. Ziegler, *J. Comput. Chem.* **2001**, *22*, 931–967.
- [36] E. van Lenthe, E. J. Baerends, *J. Comput. Chem.* **2003**, *24*, 1142–1156.
- [37] E. van Lenthe, E. J. Baerends, J. G. Snijders, *J. Chem. Phys.* **1993**, *99*, 4597–4610.
- [38] S. H. Vosko, L. Wilk, M. Nusair, *Can. J. Phys.* **1980**, *58*, 1200–1211.
- [39] M. Swart, J. G. Snijders, *Theor. Chem. Acc.* **2003**, *110*, 34–41. Erratum: *Theor. Chem. Acc.* **2003**, *110*, 111, 156.
- [40] M. Swart, P. T. van Duijnen, *Mol. Simul.* **2006**, *32*, 471–484.
- [41] N. L. Allinger, X. Zhou, J. Bergsma, *J. Mol. Struct. (THEOCHEM)* **1994**, *312*, 69–83.
- [42] J. L. Pascual-Ahuir, E. Silla, *J. Comput. Chem.* **1990**, *11*, 1047–1060.
- [43] E. Silla, I. Tunon, J. L. Pascual-Ahuir, *J. Comput. Chem.* **1991**, *12*, 1077–1088.
- [44] J. L. Pascual-Ahuir, E. Silla, I. Tunon, *J. Comput. Chem.* **1994**, *15*, 1127–1138.

Received: February 21, 2007
Published Online: June 18, 2007